Atmos. Chem. Phys. Discuss., 11, 14903–14932, 2011
www.atmos-chem-phys-discuss.net/11/14903/2011/
doi:10.5194/acpd-11-14903-2011

Atmospheric Chemistry and Physics Discussions

Fast sulfur dioxide measurements correlated with cloud concentration nuclei spectra in the marine boundary layer

D. C. Thornton[1], A. R. Bandy[1], and J. G. Hudson[2]

[1]Department of Chemistry, Drexel University, Philadelphia, PA, USA
[2]Desert Research Institute, Nevada System of Higher Education, Reno, NV, USA

Received: 2 May 2011 – Accepted: 9 May 2011 – Published: 17 May 2011

Correspondence to: D. C. Thornton (dct@drexel.edu)

Published by Copernicus Publications on behalf of the European Geosciences Union.

Abstract

During the Rain in (shallow) Cumulus over the Ocean (RICO) project simultaneous measurements of high rate sulfur dioxide (SO_2) measurements and cloud condensation nuclei (CCN) spectra were made for the first time. During research flight 14 (14 January 2005) the convective boundary layer was impacted by precipitation and ship plumes in midday but not in the late afternoon. Accumulation mode aerosols (0.14 to 0.2 µm diameter) were a factor of two greater in the latter period while CCN were 30 % to 65 % greater for aerosols that activate at supersaturations >0.1 %. Linear correlations of SO_2 and CCN were found for SO_2 concentrations ranging from 20 to 600 parts-per-trillion (pptv). The greatest sensitivities were for SO_2 and CCN that activate at supersaturations >0.1 % for both clean and polluted air. In a region affected by a cold pool event SO_2 was only linearly correlated with CCN at >0.2 % S.

1 Introduction

The Rain in (shallow) Cumulus over the Ocean (RICO) project was an intensive study of shallow cumulus clouds within the trade wind (TW) inversion (Rauber et al., 2007b). The field program was designed so that continuous radar measurements to detect precipitation were combined with intensive physical and chemical measurements obtained with several aircraft and a ship operating within the radar domain and primarily upwind of the radar site. A primary goal of RICO was to understand the conditions that exist at the onset of precipitation in the shallow cumulus clouds of the TW regime.

Several studies have considered factors that could be dominant in forming cloud drops during RICO: low level wind speeds and aerosol size distributions (Colon-Robles et al., 2006), cloud condensation nuclei (CCN) and updraft velocities (Hudson and Mishra, 2007); (Hudson et al., 2009), giant and ultragiant CCN (Arthur et al., 2010; Colon-Robles et al., 2006; Lowenstein et al., 2010; Reiche and Lasher-Trapp, 2010; Hudson et al., 2011) and the submicron sized aerosols (Lowenstein et al., 2010).

ACPD
11, 14903–14932, 2011

Gerber et al. (2008) point out these studies inferred the importance of subcloud aerosol measurements and near cloud base concentrations of droplets but neglect the processes in the upper portions of the clouds including entrainment of environmental air above the convective boundary layer (CBL).

This study presents a more detailed investigation of the subcloud aerosol distributions and their relationship to sulfur dioxide (SO_2). SO_2 is a precursor to the formation of sulfate aerosols that are considered important in forming and modifying aerosols that could become CCN as well as modifying the number concentrations and size distributions of cloud droplets. The RICO project was the first time that CCN supersaturation spectra and high rate (25 Hz sampling), continuously calibrated, high sensitivity SO_2 measurements were made simultaneously. In addition, SO_2 measurements were fast enough to estimate its flux to the surface by the eddy correlation technique. SO_2 measurements within clouds were also obtained that can be evaluated with respect to droplet concentrations.

Research flight 14 (RF14, 14 January 2005) of the National Center for Atmospheric Research (NCAR) C-130 was typical of many of the RICO C-130 flights with respect to the SO_2 concentrations. Plumes of SO_2 on the order of tens of km long were often encountered during the first circular flight track in the CBL near the surface. The most likely sources of these plumes were ships, which were observed visually on occasions but more often not. While RICO was considered "clean" for aerosol concentrations compared to continental or near shore conditions, the SO_2 concentrations were much higher than those encountered in the central Pacific CBL (Thornton et al., 1999); (Bandy et al., 1996).

The SO_2 plumes in the CBL during the early part of RF14 were remarkable in their magnitude and the areal extent. Peak CBL SO_2 concentrations reached 600 pptv and concentrations >100 pptv were pervasive in the CBL. During flight legs at 800 and 1300 m a.s.l. devoted to in situ sampling of the shallow cumulus clouds within the TW inversion, numerous encounters of SO_2 >100 pptv within the clouds were observed. In contrast, SO_2 concentrations above the CBL outside of clouds, but below the TW

Discussion Paper | Discussion Paper | Discussion Paper | Discussion Paper |

ACPD

11, 14903–14932, 2011

Fast sulfur dioxide measurements with CCN spectra

D. C. Thornton et al.

inversion, were <35 pptv except for a few short encounters with aircraft exhaust. The descriptions of the SO_2 in clouds are the subject of another paper.

2 Measurements

The suite of chemical measurements for RICO was limited in that the program was devoted to understanding the initiation of precipitation in the warm shallow cumulus clouds. The C-130 chemistry data set, in addition to SO_2, included dimethyl sulfide (DMS), ozone (O_3), water vapor, hydrogen peroxide (H_2O_2), and methyl hydroperoxide (CH_3O_2H). The sampling rates for all these gases were 25/s except for the peroxides although detector noise limited DMS data to 1/s. The C-130 physics data set included cloud condensation nucleus (CCN) counters from Desert Research Institute (DRI) (Hudson and Mishra, 2007; Hudson et al., 2009), the standard set of NCAR atmospheric state measurements, condensation nuclei (CN) counters, probes for aerosols (PCASP-200), cloud droplets (FSSP-100), and hydrometeors (260-X, 2DC, 2DP). The full suite of the instruments and measurements employed has been described in a supplement to the RICO overview paper (Rauber et al., 2007a).

The SO_2 measurements during RICO were obtained using an atmospheric pressure ionization mass spectrometer (APIMS) with continuous calibration using isotopically labeled sulfur dioxide ($^{34}SO_2$) added to the sampled air (Thornton et al., 2002). The power of this technique lies not only in the signal calibration but in the continuous indication of the performance of the APIMS in terms of sensitivity and response times under all operating conditions (Bandy et al., 1993). A blank determination was obtained using about 50 cm of 6 mm copper tubing, which removed 500 to 800 pptv SO_2 with a 1/e time of 0.58 s. Sampling at 25 Hz allows determination of SO_2 on a physical scale of 10 m. This is a great advantage for detecting SO_2 at the transitions near the cloud edges as well as variations within clouds related to the physical dynamics of the clouds. In addition, the fast response allowed detection of transients of SO_2 produced by aircraft and ship exhausts.

ACPD
11, 14903–14932, 2011

The typical C-130 flight patterns were divided between circular tracks in the CBL (Table 1) and the free troposphere (FT) regions and directed cloud sampling as frequently as possible. An initial 30 min circular track (FT1) was flown above the TW inversion in the region of interest. During this segment dropsondes were released periodically around the track to give a preview of the TW layer meteorological conditions. After descent to about 90 m above asl, a 30 min circular track (SU1, see Table 1) was flown followed by a sub cloud base circle (SC) about 450 m a.s.l. The starting locations of the CBL circles were approximately collocated and flown with opposite rotations. All the circles were advected with the mean wind with respect to the starting location.

Following the CBL circles, 3 to 4 h were devoted to sampling in and around clouds within the TW inversion. Altitudes for cloud sampling were determined by the depth of clouds for that flight with an effort to provide a representative sampling of different levels of cloud development. The remaining flight time was spent by repeating the sub-cloud base circle (SC2), a surface circle (SU2), and ascent to a final circle in the free troposphere (FT2) with dropsondes deployed as before.

3 Observations

Before an in-depth consideration of SO_2 in clouds, the chemical and physical data below cloud base were examined in the context of a well mixed CBL punctuated with the effects of precipitation. The availability of high rate data for SO_2 in conjunction with the aerosols, ozone, and thermodynamic parameters made it possible to verify that the chemical scalar quantities were responding similarly in the well mixed CBL.

With the RICO domain in the TW regime to the north and east of the Windward Islands, advection of air parcels relatively free of anthropogenic impacts from long range was expected. For RF14 the wind direction near the surface was about 075 degrees at 12 to 16 $m\,s^{-1}$ throughout the flight except near the beginning and end positions of SU1 where wind speeds were 8 to 13 $m\,s^{-1}$. The cloud layer had winds about 090 degrees at 15 $m\,s^{-1}$ except near 2 km a.s.l. where the wind speeds were

ACPD
11, 14903–14932, 2011

Fast sulfur dioxide measurements with CCN spectra

D. C. Thornton et al.

$\sim 13\,m\,s^{-1}$. At 90 m the air temperature was 25.1 °C. Ocean surface temperatures were 27 °C, except for an area near the beginning of SU1 where the surface temperature was 0.5 °C higher.

The mean O_3 was 26.5 ± 1 ppbv, except for the first half of SU1 where O_3 was periodically <25 ppbv. Positive deviations of O_3 from its mean were associated with the largest SO_2 concentrations. This indicated that sufficient time had elapsed from the combustion source that produced the SO_2 for the O_3 to recover from destruction by the large amounts of nitric oxide (NO) that would have been generated in the source. Production of O_3 then proceeds through nitrogen oxides – hydrocarbon photochemistry.

3.1 SO_2

In the free troposphere mean SO_2 was 25 pptv at the beginning of the flight (FT1) and 21 pptv near the end of the flight (FT2). These SO_2 means were statistically significant at the 95 % confidence interval. The first indication of high SO_2 concentrations in the CBL occurred on the descent in clear air to circle SU1 (Fig. 1). Mixing in the CBL brought SO_2 >100 pptv as high as 500 m a.s.l. The area bounded by 61.3° W 17.8° N and 61.8° W 18.05° N was impacted by ship plumes based on measurements 2.5 min before SU1 started through SC1 including the period between the 2 circles. The peak SO_2 concentrations near 450 s of SU1was the maximum observed although peaks over 300 pptv were observed before SU1 started and between SU1 and SC1. Because of the winds speed of $\sim 15\,m\,s^{-1}$ and the time between the encounters none of the peaks were sampled more than once. By the time the peak in SC2 was intercepted the peak in SU1 was about 40 km downwind.

Although SO_2 concentrations reached 600 pptv in the southeastern quadrant of SU1, the median SO_2 concentrations were 45 and 37 pptv for SU1 and SC1, respectively. These concentrations are more typical of the Northern Hemisphere marine CBL (Thornton et al., 1993, 1999; Tu, 2004). The northeastern quadrant of SU1 was in an area with fewer clouds overlying the track (900 to 1300 s in Fig. 2) and there was no

ACPD
11, 14903–14932, 2011

precipitation during that part of the track. The lowest SO_2 concentrations (≤30 pptv) at the end of the SU1 and SC1 circles were associated with cold pool events. The SO_2 concentrations at altitudes within the TW inversion, but above the cloud base, were <35 pptv in the absence of convected polluted CBL air and aircraft exhaust.

During the late afternoon CBL circles, mean SO_2 concentrations were 26 and 21 pptv for SU2 and SC2, respectively, which are statistically significant at the 95 % confidence interval. These mean SO_2 concentrations are typical of remote marine CBL with little contributions from anthropogenic sources (Thornton et al., 1999). One period during the SU2 circle (Figs. 2, 3, and 5 between 1200 to 1500 s) SO_2 covaried with CN and CCN. In this instance it appeared that air from a cold pool event reached 90 m a.s.l. as indicated by the anticorrelation of SO_2, CN, CCN, and O_3 with fast water vapor and equivalent potential temperature (Θ_e).

3.2 CN

A cursory inspection of the data showed similar trends in CN (CONCN variable from the C-130) and SO_2 concentrations around the circles. The time lag between these two measurements was determined to be <1 s by examining the covariance of the measurements. The correlations of CN and SO_2 were effective in indicating the pollution plumes both in time and intensity over concentrations ranges of 1 to 2 orders of magnitude.

While SO_2 measurements could be made in clouds and in precipitation events, CN data were not valid in clouds and in precipitation because of the fracturing of droplets in the inlet. Using SO_2 concentrations to indicate the pollution plumes and the responses of the NCAR FSSP-100 and the particle volume measurement (PVM) probe (Gerber Scientific) to indicate the presence of drizzle or rain, the CN data were parsed into several segments for the earlier CBL circles. During the CBL circles SU2 and SC2, precipitation was not encountered. Several brief spikes in CN during SU2 (450 s and 1700 to 1730 s) and SC2 (1740 s) where correlated with SO_2 increases although the CN spike to 500 cm^{-3} was not. The mean CN concentrations for periods not impacted

Discussion Paper | Discussion Paper | Discussion Paper | Discussion Paper |
ACPD
11, 14903–14932, 2011
Fast sulfur dioxide measurements with CCN spectra
D. C. Thornton et al.

by pollution or precipitation were significantly greater during the SU2 and SC2 circles than in the SU1 and SC1 circles (Table 2).

What is remarkable about the CN concentrations (excluding the pollution periods) are the much higher concentrations in the ending set of circles. This is in contrast to the decrease in SO_2 concentrations for the corresponding periods.

3.3 PCASP

The PCASP-200 probe was set by NCAR Research Aviation Facility to provide number concentrations in the size range 0.14 to 2.45 µm (size bins <0.14 µm were not used due to noise interference). This probe was also impacted by droplet fracturing in cloud and precipitation. The time series of the PCASP number concentrations (CONCP is the 1 s integration over the size range for valid data) also had a variation around the afternoon circles similar to CN. There was no apparent response of the PCASP to the pollution segments indicated by SO_2. This implies that the elevated CN encountered in those plumes were <0.14 µm in diameter.

The period 500 to 1200 s in each of the SU1 and SC1 circles was free of both precipitation and SO_2 plumes. The averages of the PCASP-200 number concentrations for this period clearly show that the mean CBL concentrations were nearly twice as great in the ending circles compared to the initial circles (Table 3) over approximately the same area 4 to 5 h later.

Examining the size distribution of the PCASP probe indicates that the increase in the integrated number concentrations for the later CBL circles were dominated by increases in the sizes <0.5 µm diameter (Fig. 4). Number concentrations for sizes of 0.14 to 0.2 µm (leftmost 5 bins in the spectra of Fig. 4) were twice as great in the ending CBL circles than in the earlier ones. Concentration increases of 50 to 75 % in the PCASP spectra occurred for the larger sizes in the accumulation mode (0.20 to 0.3 µm). For sizes above the peak in the accumulation mode at 0.43 µm, the concentrations were nearly equal for the early and later CBL circles (Fig. 4).

ACPD
11, 14903–14932, 2011

3.4 CCN

The CCN data (Fig. 5) were filtered in the same way as the CN because of the impacts of precipitation on the inlet. The CCN sampling and measurement response lagged the SO_2 and CN measurements by 20 to 22 s (based on covariance tests), which is accounted for in all comparisons. The CCN lag is mostly due to the time needed to activate the particles to droplets of detectable sizes within the cloud chamber but also for the air to travel to the instrument.

When the CCN data are parsed to remove the impacts of the SO_2 ship plumes, the trend for increased CCN from initial to ending CBL circles is clear for supersaturations (S) >0.1 % (Fig. 6). Higher CCN concentrations later in the day were consistent with the other aerosol data in this comparison between midday and late afternoon. The primary differences in these supersaturation spectra (Fig. 7) occurred between 0.2 % and 0.6 % S. The contributions to the increase of CCN for S >0.6 % were minimal. For CCN that activate at <0.1 % S both SU2 and SC2 had number concentrations 5 % to 30 % lower than the corresponding circles SU1 and SC1. This is remarkable considering the wind speeds of 12 to 15 $m\,s^{-1}$ during the CBL circles. Because the lowest S have the largest diameters, it would appear that salt aerosols may not have had a significant contributed to the largest CCN concentrations.

The increases in CCN concentrations at 0.2 % to 0.6 % S during SU2 and SC2 circles are consistent with the PCASP probe spectra, which had concentrations twice as great as the earlier circles for the sizes 0.14 to 0.185 µm (Fig. 4). If the CCN are primarily ammonium sulfate, the increase for CCN with 0.2 to 0.6 % S would represent particles with diameters 0.085 to 0.04 µm based on the calibration of the CCN spectrometer.

For a portion of the SU1 circle most impacted by ship exhaust, SO_2 ranged from 50 to 600 pptv with concomitant changes in CN and CCN. For the period of 400 to 500s into the circle, SO_2 and CCN were linearly correlated at all S (Fig. 8 and Table 4), although the slopes decreased with lower S. There were similar correlations between CN and CCN for this period.

ACPD
11, 14903–14932, 2011

During the SU2 circle (1100 to 1500 s, Fig. 2) SO_2, CN, and CCN displayed a synchronous variation in their concentrations. Although the variation in SO_2 was only 15 pptv about a mean of ~30 pptv, there was enough of a perturbation to assess the correlation of these three constituents. For CCN activated at 1.5 % S there was a linear correlation between SO_2 and CCN (Fig. 8; Table 4). The linear correlation between SO_2 and CCN activated at S≤0.1 % had near zero slope (Fig. 9; Table 4). The linear correlations of CN and CCN were similar to those of SO_2 and CCN.

4 Discussion

The decrease in SO_2 concentrations and the increase in number density of aerosols over a wide size range between the earlier and later CBL circles lead to the question of what impact SO_2 may have had on these aerosol number and size distributions. Several scenarios could explain these CBL observations for SO_2, CCN, CN, and the impacts of intermittent precipitation events. A well defined answer to this question cannot be obtained from RICO because the flight program was not designed for a Lagrangian process study but for a detailed study of clouds and precipitation using in situ measurements and remote sensing of the region defined by the radar domain. Consequently, the measurement space was confined to approximately the same region for each flight. Although each circle in the CBL was drifted with the wind, the starting points were approximately colocated to keep the aircraft within the radar domain for the duration of the circle. While this strategy effectively made this experiment an Eulerian one, the 4 to 5 h time step between the initial and ending CBL circles allows some inferences to be made about the CBL and evolution of aerosols as the day progressed. Given the long upwind fetch in a trade wind region of relative consistency, this may be a good assumption with regard to the chemistry and aerosol physics.

One advantage of the RICO project was that the S-band radar was running nearly continuously throughout the experimental period. In the absence of a Lagrangian mode process study, the radar data provide a look at the precipitation conditions upwind in

ACPD
11, 14903–14932, 2011

the hours prior to and during the aircraft flight. To estimate the influence that precipitation may have had on SO_2 and aerosols, every point along the CBL flight tracks was advected back in time using the *u* and *v* component winds from each second along the track to the time of the 0.5 degree radar scan. A composite of the time series of the advected tracks superimposed on the radar plots can then be viewed as movie or slide show to follow the development of the precipitation impacts.

Inspection of the time series of the back advected aircraft tracks for the SU1 and SC1 showed that the beginning and ending parts of these circles were affected by precipitation for nearly the entire time (1 to 1.5 h) the air parcels were within the radar range. The central portions of these two CBL circles were free of precipitation for the entire time the parcels were within the radar range. It was these central portions of the CBL that had higher CN and CCN concentrations (500 to 1200s into the circles in Fig. 3 top and Fig. 5a,b). These central portions of the circles give upper bounds to the aerosol concentrations while the beginning and end portions yield an estimate of the precipitation effects. However, midday mean SO_2 concentration in these central portions was 40 pptv compared to a mean of 27 pptv in the late afternoon. Because of the high water solubility of SO_2, its concentration in the midday period would be expected to have been reduced by precipitation in during SU1 and SC1. The generally higher SO_2 concentrations for the SU1 and SC1 periods likely reflected the dispersion of the ship plumes in the CBL despite any loss to precipitation.

The radar plots and the back advected tracks for the late afternoon did not indicate any precipitation for the SU2 and SC2 circles although the cloud cover was similar to the earlier CBL circles. The higher concentrations of CN, CCN activated at 0.2 to 0.4 % S, and particles sized by the PCASP during SU2 and SC2 may better represent the conditions in the absence of precipitation than the rain free portions of the SU1 and SC1 circles. Production of SO_2 during the day from DMS could have produced an SO_2 increase by late afternoon (Bandy et al., 1996; Davis et al., 1999), as was observed on some other RICO flights. During SU1 the median DMS was 87 pptv for SU1 and declined to 66 pptv during SU2. The observed medians SO_2 were 46 pptv for SU1 and

ACPD
11, 14903–14932, 2011

26 pptv for SU2. With a production efficiency of SO_2 from DMS of ~0.7 (Bandy et al., 1996), the increase in SO_2 could have been 15 pptv assuming upwind sources of DMS and the CBL conditions were similar throughout the time period.

The SO_2 fluxes estimated by eddy correlation for the first 500 s of the SU1 and SU2 circles were −0.61 and −0.36 pptv m s^{-1}, respectively. For the precipitation free central portions (750 to 1250 s) of the SU1 and SU2 circles, the SO_2 fluxes were −0.34 and −0.24 pptv m s^{-1}, respectively. The similarity in the SO_2 fluxes indicates that the loss to the surface may have been approximately equal throughout the day. For a surface flux of −0.3 pptv m s^{-1} and a 600 m CBL depth, SO_2 loss to the surface would have ~9 pptv for the 5 hr time step from SU1 to SU2.

The SC1 circle had an upward SO_2 flux of +0.51 pptv m s^{-1} for the 1000 to 1250 s portion of the circle, although the first 500 s of the circle (in the region affected by precipitation earlier) had a downward SO_2 flux of −0.36 pptv m s^{-1}. For the SC2 circle the SO_2 fluxes were +0.07 and +0.21 pptv m s^{-1}. While the periods suitable for determining SO_2 fluxes were limited on RF14 by a number of stochastic events, the SO_2 fluxes do provide some indication of fluxes of SO_2 and aerosols from the CBL during this flight.

Convection to the cloud layer was probably the primary loss mechanism of SO_2 in the CBL during SU1 and SC1. Numerous cloud penetrations during the 800 m and 1300 m flight legs had SO_2 within clouds which were over 100 pptv between 800 and 1300 m a.s.l. SO_2 was ≤35 pptv in cloud free air above the CBL when brief encounters with aircraft exhausts were excluded. With the small fluxes of SO_2 to the surface and the estimated small homogenous chemical losses, the other major loss route would have been heterogeneous processes involving aerosols.

The CCN concentrations activated at ≤0.1 % S were similar throughout the day for all the CBL circles (Fig. 6). If these CCN were sea salt, the diameters would have been in the range of 0.1 to 0.3 µm based on the in-flight calibration of the CCN spectrometer. The major change in CCN concentrations in the CBL between midday and afternoon was for CCN activated at 0.2 to 0.6 % S (Fig. 7). Although conversion of SO_2 to sulfate

ACPD
11, 14903–14932, 2011

is rapid, growth to Aitken nuclei or larger sizes takes some hours. The concentration increases in CCN activating for S >0.1 % later in the day may be due to the ∼5 h time interval between the low altitude measurements. Given the linear correlation between SO_2 and CCN activating at >0.1 % S and the absence of correlation SO_2 and CCN with ≤0.1 % S during SU2 circle (Fig. 9), those increases in CCN activating at 0.2 to 0.6 % S could be associated with SO_2 conversion to sulfate or SO_2 uptake by existing small CCN or by pre-CCN aerosols which were activated by reaction with SO_2. If larger CCN are primarily sea salt and uncorrelated to SO_2 while smaller CCN are primarily sulfates derived from SO_2, this would imply that the sulfates formed or added to the smallest CCN would impact cloud formation if the supersaturations in the clouds were much greater than 0.1 % S (Hudson et al., 2010).

The large increase in number concentration, as well as mass, in the accumulation mode <0.4 µm indicated by the PCASP spectra. It is unlikely that this large increase was due to any homogeneous or heterogeneous processes in the CBL within the ∼5 h time between SU1 and SU2. Most likely heterogeneous processes over a number of days would have produced this result. Precipitation averaged over the radar domain during RICO was typically <10 % with an estimate of ∼15 % for RF14 (Rauber et al., 2007b; Snodgrass et al., 2009).

In the absence of precipitation, reprocessing of evaporated cloud drops and aerosols followed by entrainment into the CBL from the cloud layer maybe the source of the increase of the accumulation mode aerosols (Lasher-Trapp et al., 2005). An example of this may be seen in the period of 1100 to 1600 s of SU2 where there was a synchronous variation of SO_2, CN, and CCN (Figs. 2, 3, 5). Based on Θ_e this period appeared to be the result of a cold pool event reaching as low as 90 m a.s.l. This is further supported by increases in O_3 to concentrations typical of the 800 and 1100 m flight legs. Ozone covaried with SO_2, CN, and CCN although with a lag time of unknown origin. Because O_3 is destroyed in the CBL, the O_3 increases must have been from entrainment of air from above the CBL.

ACPD
11, 14903–14932, 2011

An alternative scenario could be that the SU1 and SC1 concentrations of CCN with 0.2 to 0.4 % S were reduced by convection into the clouds during the early morning and midday. Hudson et al. (2009) found that cloud drop concentrations were well correlated to CCN activated at 1 % S for the surface flight levels. This S is probably similar to S of most RICO cumulus clouds because Hudson et al. (2010) found S values of nearly 1 % in stratus clouds with similar low droplet concentrations to RICO. Cumulus clouds have higher updrafts, which should produce higher S. Taking the effective S (S_{eff}) as number of CCN that activate at 1 % S equal the number of cloud drops (N_c) near cloud base, the mean S_{eff} for the surface circles during RICO was 0.5 % with a range of 0.2–1.5 % S. This is similar to the range found for stratocumulus cloud decks with mean CCN that activate at 1 % S (Hudson et al., 2010).

5 Conclusions

During RICO RF14 there was dichotomy of conditions below cloud base between the midday period and the late afternoon period. The midday CBL had concentrations of SO_2 > 100 pptv from ship exhausts in a region with significant precipitation. Upwind of the precipitation region, there were ~50 % lower CCN number density at S>0.1 %, ~50 % lower number density of aerosols with diameters of 0.14 to 0.2 µm compared to the late afternoon for the same region. In the ship exhaust plumes, SO_2 concentrations >100 pptv were linearly correlated with CCN over the entire range of measured supersaturations, although the magnitudes of the slopes were lower for CCN activated at <0.2 % S compared to higher S. The lower concentrations of CCN and aerosols ≤0.2 µm may have been the result of cloud processing without precipitation despite the high SO_2 concentrations that could have generated considerable sulfate aerosols. The lower concentrations of CCN that activate at 0.2 to 0.4 % S observed during the midday period could be associated with cloud formation and precipitation, but likely represent the steady state condition and not the initial state.

ACPD
11, 14903–14932, 2011

In the late afternoon when the mean CBL SO_2 was 26 pptv (standard deviation ±6 pptv), SO_2 was linearly correlated with CCN that activate at supersaturations >0.2 %, but there was no correlation with CCN that activate <0.2 % S. A cold pool event appeared to have a significant role in bringing into the CBL aerosols that were processed in clouds. The ~50 % greater number densities of CCN that activate with >0.2 % S during the late afternoon period may have contributed to formation of clouds in which precipitation was not favored due to the higher number density of CCN. Models using the late afternoon condition as input may answer this question.

Given the conditions that were observed during the midday, the question remains: did the measured CCN spectra during the midday represent the end result of cloud formation and precipitation and did the late afternoon measured CCN spectra represent the CBL conditions with cloud formation but without precipitation? Since precipitation was frequently observed early in the day during RICO and that SO_2 from ship plumes was frequently observed in the first CBL circles, the impact of SO_2 on cloud formation and precipitation remains poorly understood and deserves further study from measurements and modeling.

Acknowledgements. Support from the National Science Foundation under grants ATM-0342138, ATM-0627227, ATM-0627227, and ATM-0342618 is gratefully acknowledged. National Center for Atmospheric Research (NCAR) is sponsored by the National Science Foundation. We thank the NCAR Research Aviation Facility for their assistance throughout the C-130 operation phase of RICO. Data from the RICO project archive at NCAR Earth Observing Laboratory archive for data obtained on the C-130 and the Radar Image Archive for the radar images for RF14 are gratefully acknowledged.

References

Arthur, D. K., Lasher-Trapp, S., Abdel-Haleem, A., Klosterman, N., and Ebert, D. S.: A new three-dimensional visualization system for combining aircraft and radar data and its application to RICO observations, J. Atmos. Oceanic Tech., 27, 811–828, doi:10.1175/2009JTECHA1395.1, 2010.

ACPD

11, 14903–14932, 2011

Bandy, A. R., Thornton, D. C., and Driedger, A. R.: Airborne measurements of sulfur dioxide, dimethyl sulfide, carbon disulfide, and carbonyl sulfide by isotope dilution gas chromatography mass spectrometry, J. Geophys. Res.-Atmos., 98, 23423–23433, 1993.

Bandy, A. R., Thornton, D. C., Blomquist, B. W., Chen, S., Wade, T. P., Ianni, J. C., Mitchell, G. M., and Nadler, W.: Chemistry of dimethyl sulfide in the equatorial Pacific atmosphere, Geophys. Res. Lett., 23, 741–744, 1996.

Colon-Robles, M., Rauber, R. M., and Jensen, J. B.: Influence of low-level wind speed on droplet spectra near cloud base in trade wind cumulus, Geophys. Res. Lett., 33, L20814, doi:10.1029/2006GL027487, 2006.

Davis, D., G., C., Bandy, A., Thornton, D., Eisele, F., Mauldin, L., Tanner, D., Lenschow, D., Fuelberg, H., Huebert, B., Heath, J., Clarke, A., and Blake, D.: Dimethyl sulfide oxidation in the equatorial Pacific: comparison of model simulations with field observations for DMS, SO_2, H_2SO_4(g), MSA(g), MS and NSS, J. Geophys. Res.-Atmos., 104, 5765–5784, 1999.

Gerber, H. E., Frick, G. M., Jensen, J. B., and Hudson, J. G.: Entrainment, mixing, and microphysics in trade-wind cumulus, J. Meteorol. Soc. Jpn., 86, 87–106, 2008.

Hudson, J. G. and Mishra, S.: Relationships between CCN and cloud microphysics variations in clean maritime air, Geophys. Res. Lett., 34, L16804, doi:10.1029/2007GL030044, 2007.

Hudson, J. G., Noble, S., Jha, V., and Mishra, S.: Correlations of small cumuli droplet and drizzle drop concentrations with cloud condensation nuclei concentrations, J. Geophys. Res.-Atmos., 114, D05201, doi:10.1029/2008JD010581, 2009.

Hudson, J. G., Noble, S., and Jha, V.: Stratus cloud supersaturations, Geophys. Res. Lett., 37, L21813,doi:10.1029/2010gl045197, 2010.

Hudson, J. G., Jha, V., and Noble, S.: Drizzle correlations with giant nuclei, Geophys. Res. Lett., 38, L05808 doi:10.1029/2010gl046207, 2011.

Lasher-Trapp, S. G., Cooper, W. A., and Blyth, A. M.: Broadening of droplet size distributions from entrainment and mixing in a cumulus cloud, Q. J. Roy. Meteor. Soc., 131, 195–220, doi:10.1256/qj.03.199, 2005.

Lowenstein, J. H., Blyth, A. M., and Lawson, R. P.: Early evolution of the largest-sized droplets in maritime cumulus clouds, Q. J. Roy. Meteor. Soc., 136, 708–717, doi:10.1002/qj.597, 2010.

Rauber, R. M., Stevens, B., Ochs, H. T., Knight, C., Albrecht, B. A., Blyth, A. M., Fairall, C. W., Jensen, J. B., Lasher-Trapp, S. G., Mayol-Bracero, O. L., Vali, G., Anderson, J. R., Baker, B. A., Bandy, A. R., Burnet, E., Brenguier, J. L., Brewer, W. A., Brown, P. R. A., Chuang, P., Cotton, W. R., Di Girolamo, L. D., Geerts, B., Gerber, H., Goke, S., Gomes, L., Heikes, B. G., Hudson, J. G., Kollias, P., Lawson, 5 R. P., Krueger, S. K., Lenschow, D. H., Nuijens, L., OSullivan, D. W., Rilling, R. A., Rogers, D. C., Siebesma, A. P., Snodgrass, E., Stith, J. L., Thornton, D. C., Tucker, S., Twohy, C. H., and Zuidema, P: Electronic supplement to Rain in (shallow) Cumulus over the Ocean–The RICO campaign, Bull. Am. Meteorol. Soc., 88, S12–S18, 2007a.

Rauber, R. M., Stevens, B., Ochs, H. T., Knight, C., Albrecht, B. A., Blyth, A. M., Fairall, C. W., Jensen, J. B., Lasher-Trapp, S. G., Mayol-Bracero, O. L., Vali, G., Anderson, J. R., Baker, B. A., Bandy, A. R., Burnet, E., Brenguier, J. L., Brewer, W. A., Brown, P. R. A., Chuang, P., Cotton, W. R., Girolamo, L. D., Geerts, B., Gerber, H., Goke, S., Gomes, L., Heikes, B. G., Hudson, J. G., Kollias, P., Lawson, R. P., Krueger, S. K., Lenschow, D. H., Nuijens, L., O'Sullivan, D. W., Rilling, R. A., Rogers, D. C., Siebesma, A. P., Snodgrass, E., Stith, J. L., Thornton, D. C., Tucker, S., Twohy, C. H., and Zuidema, P.: Rain in shallow cumulus over the ocean – The RICO campaign, Bull. Am. Meteorol. Soc., 88, 1912–1928, 2007b.

Reiche, C. H. and Lasher-Trapp, S.: The minor importance of giant aerosol to precipitation development within small trade wind cumuli observed during RICO, Atmos. Res., 95, 386–399, 2010.

Snodgrass, E. R., Di Girolamo, L., and Rauber, R. M.: Precipitation characteristics of trade wind clouds during RICO derived from radar, satellite, and aircraft measurements, J. Appl. Meteorol. Climatol., 48, 464–483, 2009.

Thornton, D. C., Bandy, A. R., Beltz, N., Driedger, A. R., and Ferek, R.: Advection of sulfur dioxide over the western Atlantic Ocean during CITE-3, J. Geophys. Res.-Atmos., 98, 23459–23467, 1993.

Thornton, D., Bandy, A., Blomquist, B., Driedger, A., and Wade, T.: Sulfur dioxide distribution over the Pacific Ocean 1991–1996, J. Geophys. Res.-Atmos., 104, 5845–5854, 1999.

Thornton, D., Bandy, A., Tu, F., Blomquist, B., Mitchell, G., Nadler, W., and Lenschow, D.: Fast airborne sulfur dioxide measurements by atmospheric pressure ionization mass spectrometry (APIMS), J. Geophys. Res.-Atmos., 107, 4632 doi:4610.1029/2002JD002289, 2002.

Tu, F. H., Thornton, D. C., Bandy, A. R., Carmichael, G. R., Tang, Y., Thornhill, K. L., Sachse, G. W., and Blake, D. R.: Long-range transport of sulfur dioxide in the central Pacific, J. Geophys. Res.-Atmos., 109, D15S08, doi:10.1029/2003JD004309, 2004.

ACPD
11, 14903–14932, 2011

Fast sulfur dioxide measurements with CCN spectra

D. C. Thornton et al.

Table 1. Start times of CBL circles for RICO RF14.

SU1	Initial surface circle at 90 m	16:12:19 UTC*
SC1	Initial sub-cloud circle at 450 m	16:49:04 UTC
SU2	Final surface circle at 90 m	21:46:39 UTC
SC2	Final sub-cloud circle at 450 m	21:09:49 UTC

* Local time is UTC-4.

ACPD
11, 14903–14932, 2011

Table 2. NCAR CN number concentrations for the CBL circles of RICO RF14. Differences in means between initial circles and later circles were significant at the 95 % confidence interval.

Circle	Time into circle	Mean (#/cc)	Std. dev. (#/cc)	Std. err. of mean (#/cc)	*n*
SU1	901 to 1200 s	245.4	5.57	0.32	300
SU2	1 to 250 s	282.1	5.1	0.32	250
SU2	501 to 750 s	302.5	7.02	0.44	250
SC1	980 to 1200s	218.4	6.05	0.41	221
SC2	1 to 250 s	249.1	4.47	0.28	250
SC2	501 to 750 s	282.9	4.94	0.31	250

ACPD
11, 14903–14932, 2011

Table 3. Statistics for the PCASP-200 number concentrations for sizes 0.14 to 2.75 µm integrated for 1 s for the precipitation free period 500 to 1200 s ($n = 701$) into the circles.

Circle	Mean (#/cc)	Std. dev. (#/cc)	Std. error of mean (#/cc)
SU1	35.4	7.11	0.27
SU2	69.1	10.5	0.40
SC1	37.5	6.79	0.26
SC2	65.2	9.13	0.34

ACPD
11, 14903–14932, 2011

Table 4. Linear regressions of CCN on SO_2 or CN for two CBL events. Period 395 to 475 s was a pollution event ($n = 24$). Period 1200 to 1500 s was in a cold pool event ($n = 66$).

	SO_2				CONCN			
	SU1		SU2		SU1		SU2	
	395 to 475 s		1200 to 1500 s		395 to 475 s		1200 to 1500 s	
Supersaturation	1.5 %	0.1 %	1.5 %	0.1 %	1.5 %	0.1 %	1.5 %	0.1 %
Slope	1.35	0.73	1.61	0.073	0.60	0.31	0.61	0.06
Std. dev of slope	0.08	0.08	0.32	0.22	0.05	0.05	0.11	0.08
Correlation coeff.	0.96	0.89	0.53	0.04	0.92	0.82	0.58	0.10

ACPD
11, 14903–14932, 2011

Fast sulfur dioxide measurements with CCN spectra

D. C. Thornton et al.

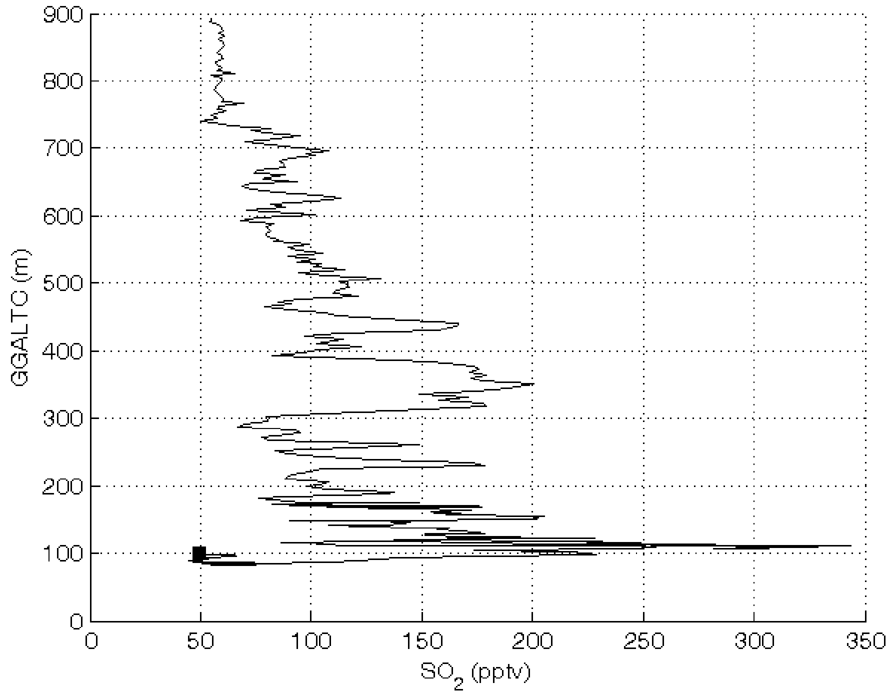

Fig. 1. Portion of the C-130 descent in clear air to the start of the first surface circle (filled square). SO_2 >100 pptv from probable ship plumes was mixed to 500 m a.s.l. Data obtained at 25 samples/s were integrated to 1/s.

ACPD
11, 14903–14932, 2011

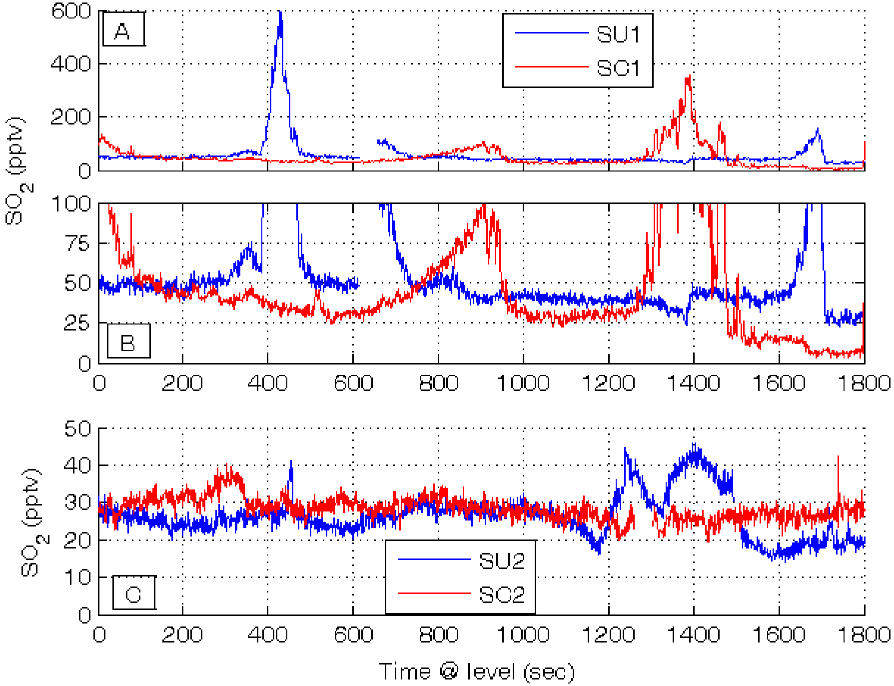

Fig. 2. SO_2 (1 Hz) time series for CBL circles of RICO F14. **(B)** shows an expanded scale of **(A)**. Times are relative to the start times of circles given in Table 1. The SO_2 peak near 1400 s of SC1 is not the same one as the peak in near 450 s of SU1, which was 40 km downwind at the time of the peak in SC1.

ACPD
11, 14903–14932, 2011

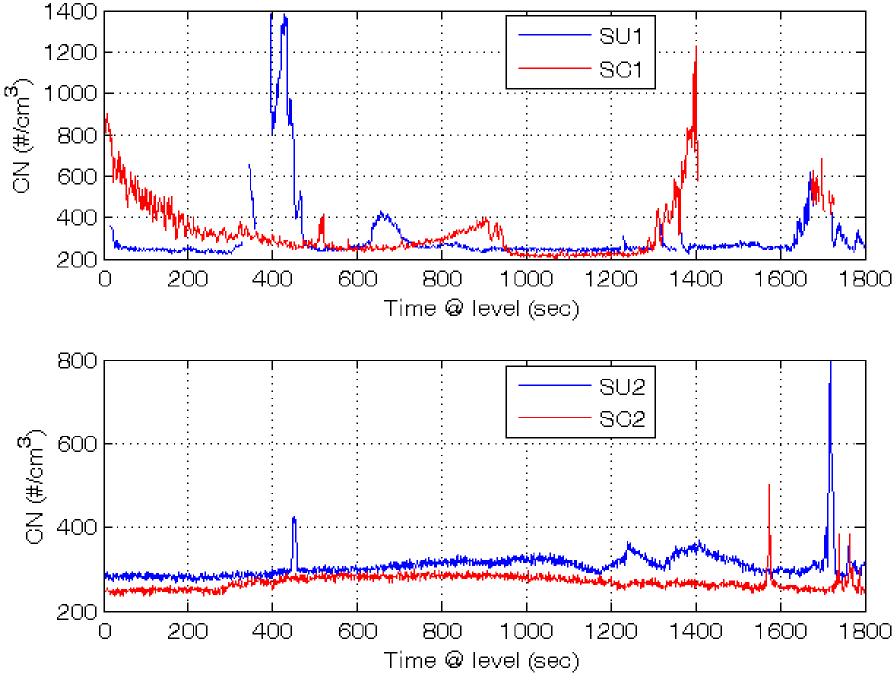

Fig. 3. Time series of NCAR C-130 CN for CBL circles of RICO RF14 without periods of precipitation interference.

ACPD
11, 14903–14932, 2011

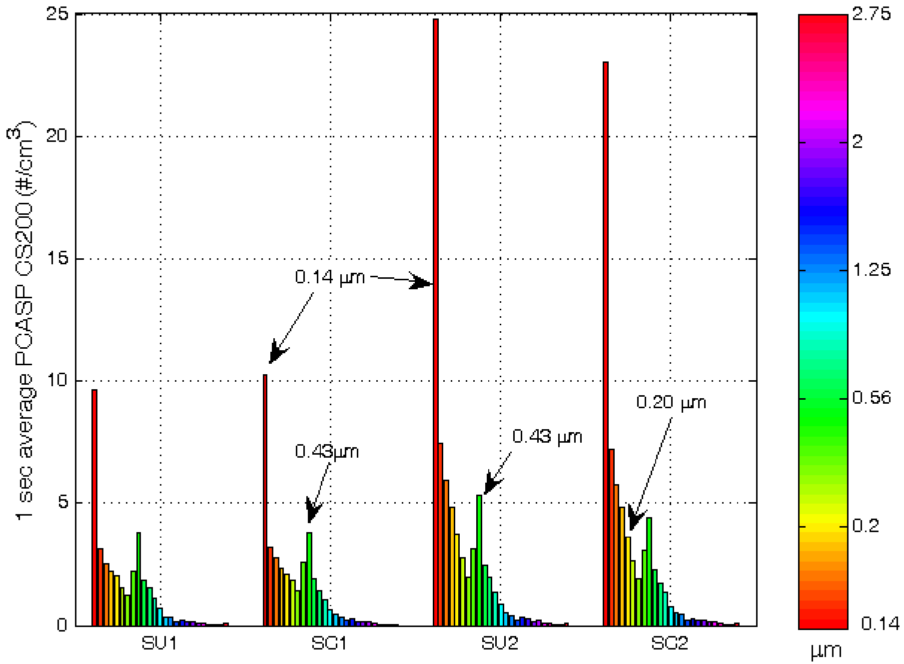

Fig. 4. Size spectra from 10 Hz PCASP-200 integrated over the 500 s to 1200 s portions of the CBL circles of RICO RF14 excluding the periods of precipitation.

ACPD
11, 14903–14932, 2011

Fast sulfur dioxide measurements with CCN spectra

D. C. Thornton et al.

Title Page
Abstract | Introduction
Conclusions | References
Tables | Figures
◀I | ▶I
◀ | ▶
Back | Close
Full Screen / Esc
Printer-friendly Version
Interactive Discussion

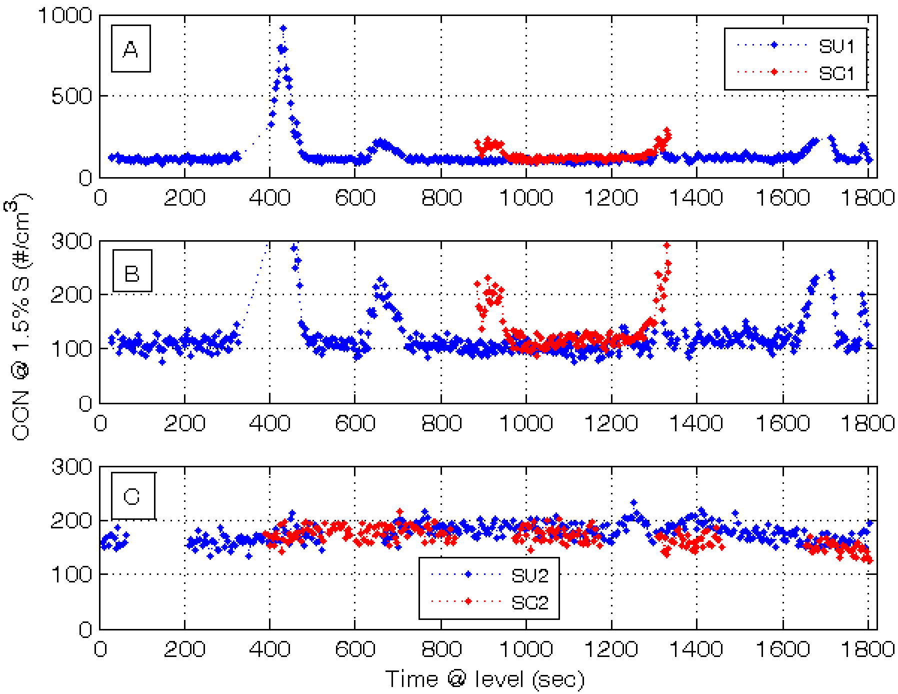

Fig. 5. Cumulative CCN at 1.5 % supersaturation for the CBL circles of RICO RF14 excluding the periods of precipitation. **(B)** shows an expanded scale of panel **(A)**.

ACPD
11, 14903–14932, 2011

Fast sulfur dioxide measurements with CCN spectra

D. C. Thornton et al.

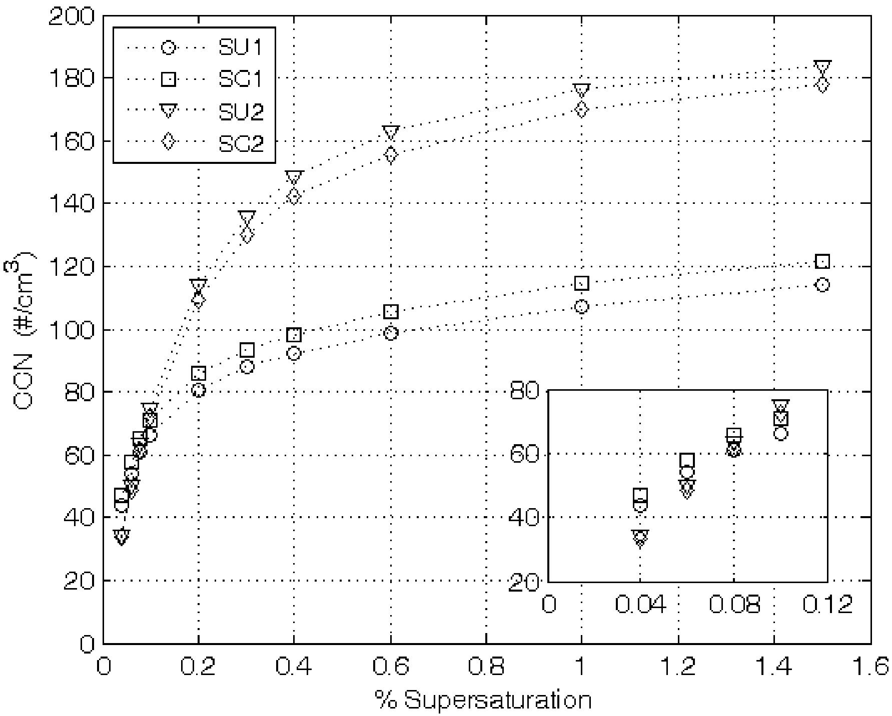

Fig. 6. Mean CCN cumulative concentrations as a function of supersaturation from the 4 CBL circles for periods free of SO_2 pollution and precipitation. Circles SU1, SU2, and SC2 had several segments which were aggregated for the means for those circles. Circle SC1 had limited data compared to the other circles.

ACPD
11, 14903–14932, 2011

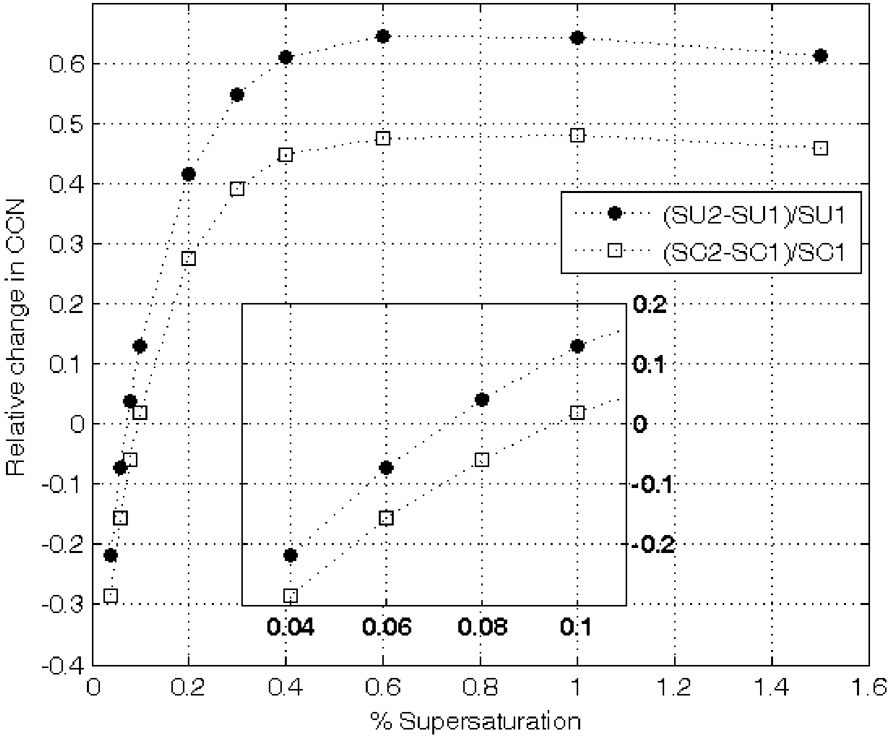

Fig. 7. Change in the cumulative CCN means for the late afternoon circles relative to the midday circles.

ACPD
11, 14903–14932, 2011

Fast sulfur dioxide measurements with CCN spectra

D. C. Thornton et al.

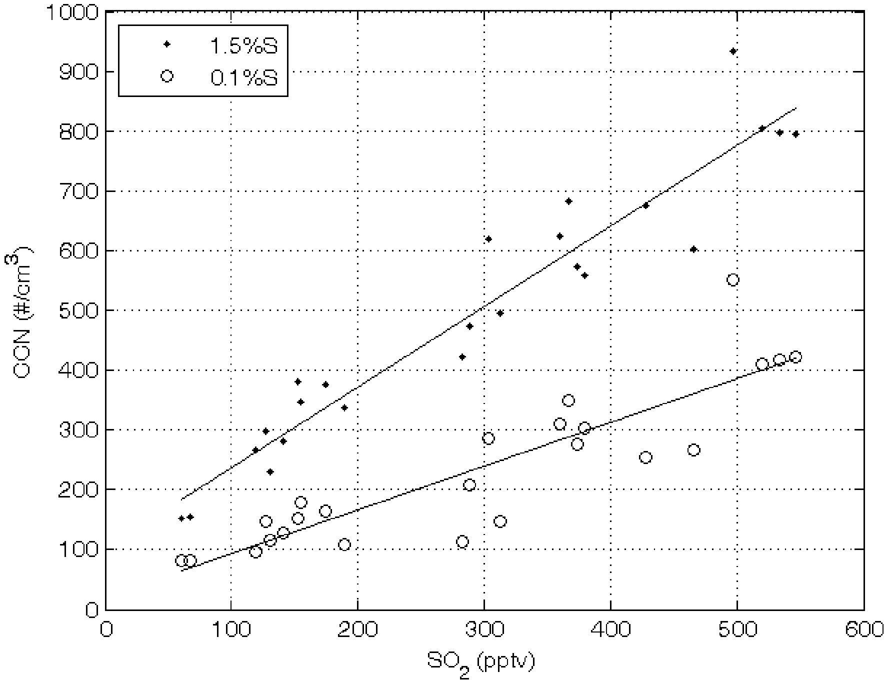

Fig. 8. Regression of CCN on SO_2 in a pollution plume from 400 s to 500 s of circle SU1.

ACPD
11, 14903–14932, 2011

Fast sulfur dioxide measurements with CCN spectra

D. C. Thornton et al.

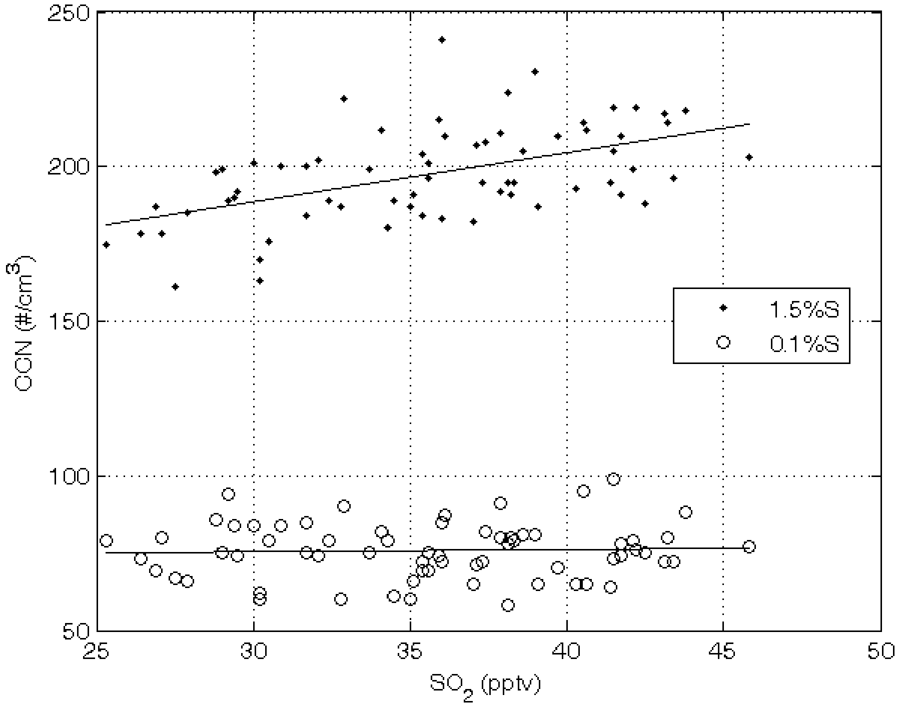

Fig. 9. Regression of CCN on SO_2 for 1200 s to 1500 s of circle SU2 which was affected by a cold pool event.

ACPD
11, 14903–14932, 2011

Fast sulfur dioxide measurements with CCN spectra

D. C. Thornton et al.